The advances in surface roughness effects studies in transportation industries

ZAMBRI HARUN[1]*, BAGUS NUGROHO[2,3], LEON CHAN[4] AND SOHIF MAT[5]

[1]*Department of Mechanical and Material Engineering, Universiti Kebangsaan Malaysia, 43600 Bangi, Malaysia*
[2]*Aerodynamics and Flight Mechanics Group University of Southampton, Southampton, SO17 1BJ, UK*
[3]*Department of Mechanical Engineering, University of Melbourne, Victoria, 3010, Australia*
[4]*Department of Mechanical Engineering, Universiti Tenaga Nasional, 43000 Kajang, Malaysia*
[5]*Solar Energy Research Institute (SERI), Universiti Kebangsaan Malaysia, 43600 Bangi, Malaysia*
**zambri@ukm.edu.my*

ABSTRACT

Aerodynamic and skin friction effects are two main factors determining fuel efficiencies in the transportation industry. In any of transportation areas, either road transport, railway, maritime or aerospace, fuel efficiency has become interesting and sometimes sensitive topics. In this article, the authors collect information and analyze recent trend in surface roughness technology to overcome one of the factors in fuel efficiency, i.e. skin friction. The study collects data from experimental studies, simulations as well as news and discussions in engineering bulletins. World largest economies are securing their maritime trade routes to protect their economies as fuels used in large tankers are directly proportional to travel distance. Studies in skin friction are very important because skin friction drag account the majority of drag in large tankers. The use of biomimetic, the study of the structures and functions of biological systems in the design of engineering systems have attracted a lot of attentions in the last few decades. Mimicking the nature such as the arrangement and pattern on shark scales and how owls quietly fly have contributed to progress in various engineering fields. Simulation works are carried out especially to reduce costs and to obtain estimation of drags prior to experiment works. However, current computational resources only allow turbulent flows to be simulated at low and medium Reynolds numbers—far below that of engineering flows. This has lead researchers to use develop empirical models which can be used for practical engineering applications so that engineers are able to obtain a quick estimate of the drag penalty of the surface. Throughout the years, many models have been proposed but none has been universally reliable. Indeed, the turbulent flow over rough surfaces is a complex field of research and much is still to be discovered.

Keywords: Surface roughness, Skin friction

INTRODUCTION

There have been a lot of technological advancements in developing energy efficient vehicles or systems, such as the lighter composite and more fuel-efficient jet engines for aviation industry, energy efficient vehicles by employing hybrid technology, using electric motors and hydrogen fuel cells for automotive industry and many more. Although these efforts have been helpful, there is room for improvement to reduce drag by controlling surface turbulence. Skin-friction drag comes from a thin region of slow moving fluid immediately adjacent to a solid surface. Energy consumption to overcome skin-friction drag is relatively costly, for example: around 50% of the total drag in modern aircraft is caused by skin-friction drag (Saric et al. 2011, Lee et al. 2011, Stenzel et al. 2011), in large ship such as container ship and very large crude carrier (VLCC), it is up to 80%. The issue of skin friction drag is made worse with the existence of surface roughness. Uneven wall such as biofouling on ship hull, rivets on aircraft fuselage, and window joints on high speed train contributes to an increase in drag penalty.

One method to overcome skin drag is by controlling the turbulence levels on the surface. Riblets is one of the most popular method to control the near wall structures. It is inspired from shark skin and has been tested in various engineering applications such as yatch, swimming suit and aircraft (Dean & Bhushan 2010). Recently however, Marusic et al. 2010 and Smits & Marusic 2013 show that at high Reynolds number (where most engineering systems run), small-scale structures are dominated by large-scale features that reside further away from the wall. It is believed that large features may influence the near-wall structures, which are directly correlated to the skin friction drag. Hence, many researches are now looking at ways to control large-scale features. One such method is by modify regular riblets into herringbone pattern (see Harun et al. 2016, Koeltzsch et al. 2002, Nugroho et al. 2013). Early result shows that this directional riblet pattern can capture and lock the large-scale structure. Further studies are currently still underway, particularly the one that lead to drag reduction mechanism.

MULTI-BILLION STRATEGIC INVESTMENTS IN PORT INDUSTRY AND SECURING MARITIME ROUTES

The potential of surface roughness feature to be used, is large and can be very beneficial to the econimy. The possibility of using riblets to reduce drag and subsequently decrease fuel consumption is very tantalizing. For a country like Malaysia who relies heavily on sea transportation for trade with other countries, and subsequent investment in large ports, a slight increase in transportation efficiency could result in billions of savings. In this region, it makes a lot of sense for countries like the United States, China and India to rationalise their trade routes as the travel distance is very important aspect in cargo transportation. The second biggest economy in the world, China, is very ambitious about securing sea routes. China through its government-backed companies invest heavily in Malaysia, Sri Lanka and the Philippines.

The geographical location of Malaysia gives it the upper hand advantage to attract the use of ports around the country. The Strait of Malacca, which runs between Indonesia, Malaysia and Singapore, has long been a major gateway for trade to and from Asia, and is once again rapidly rising in importance. It is now the world's number two busiest waterway after the Strait of Hormuz. Last year sees Port Klang, the twelfth busiest port in the world, handling 31.2 TEUs (twenty-foot equivalent unit), a rise of 10.8% over 2015. In comparison, the Port of Singapore handled 30.9 million TEUs in 2015. The country has already embarked upon completing the Kuantan Port and its industrial park. Malaysian Transport Minister Mr. Liow Tiong Lai was reported mentioning that the expansion of Kuantan Port into a deepwater port is expected to be completed by next year (2018). Once completed, the port will be able to accommodate Cape-sized vessels and post-Panamax container ships of up to 200,000 deadweight tonnes (DWT) (Khoo 2016). DWT is a measurement of how much weight a ship can safely carry. Currently, the container part of the port of Kuantan could only handle ships of up to 35,000 DWT. The majority i.e. 49% belongs to the Chinese consortium led by the state-owned conglomerate Guangxi Beibu Gulf International Port Group and the rest by Malaysian various government agencies and companies. Chinese dependence on ports built in Malaysia especially for its energy supply from Saudi and Iran is much more pronounced when more of its government-link agencies are tying up with Malaysian counterparts to build more ports i.e. Port of Malacca and recently the estimated (RM) one-trillion

gross development value (GDV) for Carey Island Port development and its and related infrastructure, industrial parks and free trade zones (Foon 2017).

Opportunities like this should not be missed, nevertheless many express more balance should be made because these infrastructures are strategic for national securities. The United States and the Australian governments have in the past blocked purchases of their respective ports by Chinese business entities. In Sri Lanka, part of the country push to reduce debt is to construct a port city and its real estates near Colombo by Chinese backed companies. The US$1.4 billion Port City project by China Communication Construction Company (CCCC) started late last year as part of Beijing's ambitious plans to create a modern-day "Silk Road" across Asia. The Port City built on reclaimed land, will see a total investment of $USD13bn in the form of housing, marinas, health facilities, schools and other developments over the next 30 years. Objections from India, due to strategic issue, caused Prime Minister Sirisena's administration to reject a proposal to give 20 hectares of freehold land to only on a 99-year lease to CCCC.

There are a few other reasons where countries in this region should view opportunities with different perspectives or rather cautions e.g. congestions as overcrowding causes accidents. Recent accident in September 2016 near Port of Tanjung Pelepas caused major oil spills in Malaysia (Igaz 2016). Attracting supertankers and VLCCs might end up destroying local marine ecosystem.

Emissions are related to fuel usage and performance, when the vehicles need to go faster or carry more load, more emissions are released. The true scale of climate change emissions from shipping is almost three times higher than previously believed, according to a leaked UN study seen by The Guardian in 2008. It calculates that annual emissions from the world's merchant fleet have already reached 1.12bn tonnes of Carbon Dioxide (CO_2), or nearly 4.5% of all global emissions of the main greenhouse gas. The report suggests that shipping emissions - which are not taken into account by European targets for cutting global warming - will become one of the largest single sources of manmade CO_2 after cars, housing, agriculture and industry (The Guardian 2016).

FUNDAMENTAL THEORY

Turbulent boundary layer is a small thin region of low velocity fluid immediately adjacent to a solid surface with certain thickness, δ. This region arises from no-slip condition at the wall/boundary where the velocity gradient generates skin-friction drag. Skin-friction drag is the force that ship, aircraft and cars propulsion system need to overcome to move forward. For a passenger car, a 5% contribution from total drag due to skin is considered high. Most of the drag is contributed by the form drag or aerodynamic drag. A passenger car can be categorized as a bluff body. For a large marine vehicle such as ship, the energy to overcome skin friction drag is high. As mentioned earlier, for a large ship such as a VLCC, around 80% of the total drag is due to skin friction. VLCC can be categorised as a streamlined body.

For a turbulent flow over smooth surface or flat plate, the flow can be divided into two regions, namely inner layer and outer layer. The term inner layer is generally used to describe flow close to the wall where viscosity dominate, while the outer layer is applied to define flow that is further from the wall where inertia has more role (Smits et al, 2010).

In wall bounded turbulent flow the location where inner and outer region overlap is commonly termed as logarithmic region, where the mean velocity *U* follows a logarithmic profile over certain wall-normal distance *z*:

$$U^+ = \frac{1}{\kappa} log(z^+) + A \quad (1)$$

Here $U^+ = U/U_\tau$, where U_τ is skin friction velocity, A is log-law intercept, κ is von Karman, and $z^+ = zU_\tau/\nu$, where ν is kinematic viscosity constant (Clauser 1954; Perry & Li 1990). Here U_τ can also be defined as $\sqrt{\tau_w/\rho}$ where τ_w is wall shear stress and ρ is the fluid density. The skin-friction velocity U_τ is proportional to the skin-friction drag, in other words higher skin-friction velocity resulting in higher skin-friction drag. Figure 1 shows mean velocity profile of typical turbulent boundary layer over smooth wall.

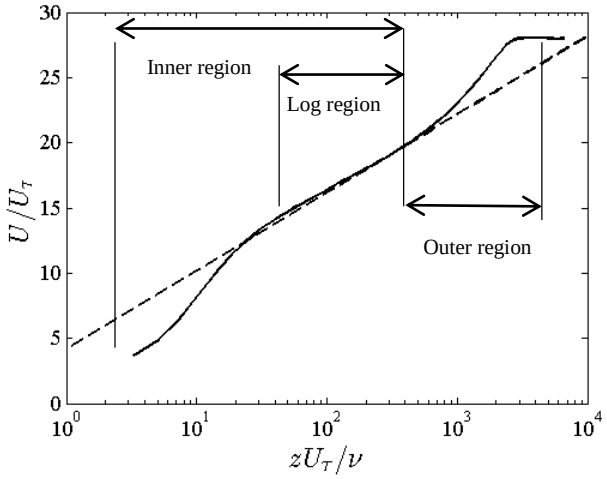

FIGURE 1. Velocity profile from turbulent boundary layer over smooth wall (Nugroho et al. 2013)

EXPERIMENTAL STUDIES ON TURBULENT BOUNDARY LAYER OVER ROUGH WALL

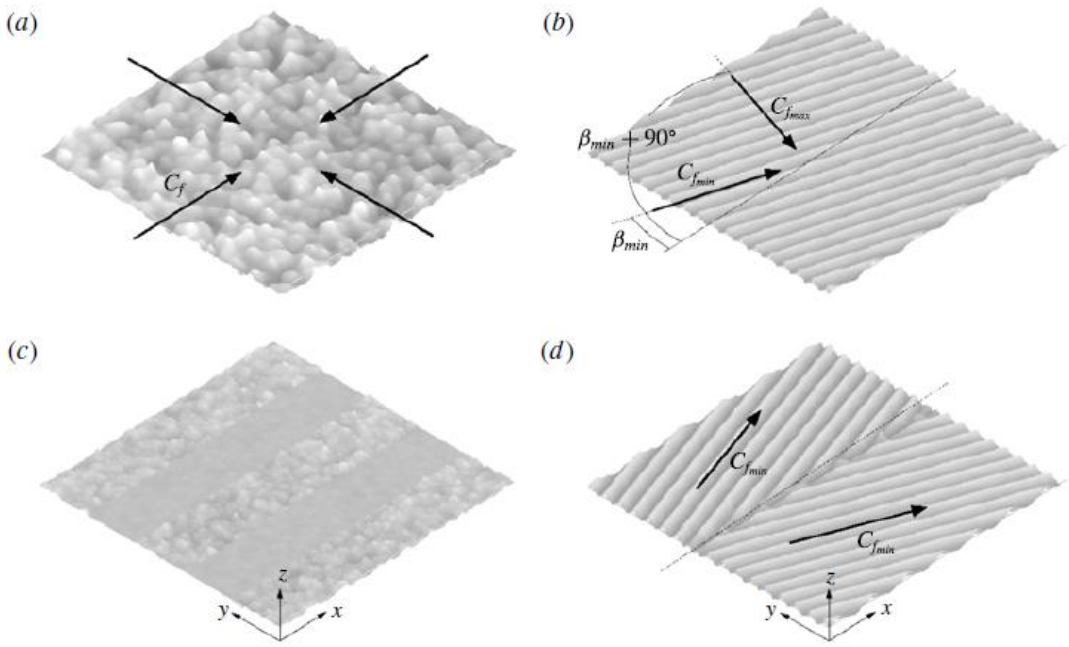

FIGURE 2: Various roughness types (Kevin et al, 2017).

The issue of skin friction drag is exacerbated with the existence of rough surface. Currently there are plethora types of roughness study available in literature, such as: sand paper grit (Nikuradse 1933; Amir & Castro, 2011; Squire et al. 2016a; 2016b), wire mesh (Archarya et al, 1986; Perry and Li, 1990; Krogstad and Antonia 1999), uniform spheres (Ligrani and Moffat, 1986; Acharya et al. 1986), transverse rectangular blocks (Perry et al. 1969; Volino et al., 2009), etc. To simplify the various type of roughness, Kevin et al (2017) shows that it can be categorised into four different type of roughness (refer to figure 2).

TABLE 1: Type of surface roughness categorised in Figure 2

Figure 2	Local C_f (Coefficient of friction) isotropy	C_f (Coefficient of friction) distribution
a	Isotropic	Homogeneous
b	Anisotropic	Homogeneous
c	Isotropic	Heterogeneous
d	Anisotropic	Heterogeneous

The effect of roughness can be observed on the mean velocity profile, where it causes a vertical downward shift on the log profile due to ΔU^+ or Hama roughness function. The log-law profile is given as

$$U^+ = \frac{1}{\kappa} log(z^+) + A - \Delta U^+ \quad (2)$$

where $\Delta U^+ = U/U_\tau$. Figure 3 shows the mean velocity profile over rough wall where it experience vertical shift down due to rough surface.

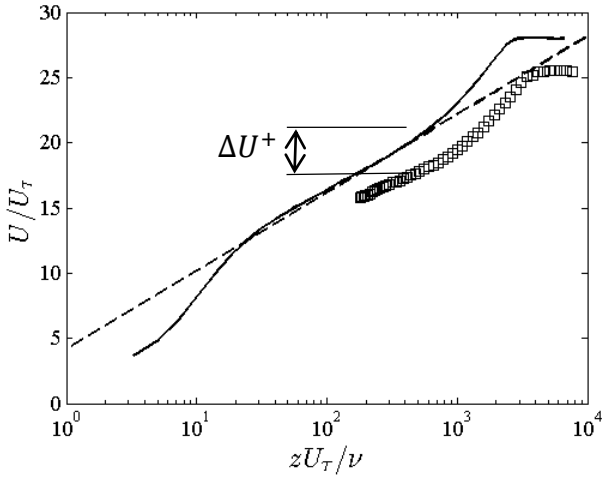

FIGURE 3: Flow over rough and smooth wall

For turbulent boundary layer over rough wall there is another parameter needed to estimate drag, which is k_s, or equivalent sand grain roughness height (Nikuradse, 1933). Although the unit of k_s is in meter, it is not a quantity that can be measured directly. It is a flow measure features that show the quantity of the effect that the roughness has on the turbulent boundary layer. k_s can be estimated by exposing the rough surface to turbulent flow at different Reynolds number. Currently, the most common technique to estimate k_s is through wind tunnel via hot-wire and drag-force balance (Monty et al, 2016; Baars et al, 2016; Squire et al, 2016a; 2016b) or towing tank-experiment (Schultz, 2004; 2007) where we assume "fully rough" condition in the form of:

$$\Delta U^+ = \frac{1}{\kappa} log(k_s^+) + A - B \quad (3)$$

here k_s^+ can also be translated as $k_s U_\tau / v$.
The challenge in finding k_s is the relatively high cost, in term of experiment resources and time. A fluid dynamicist would need to perform many rough surface wall-normal measurements at various Reynolds number to obtain several ΔU^+ values.

LABORATORY ROUGHNESS EXPERIMENTS

In this section the authors report some recent and upcoming investigations of rough surface on marine vehicle from The University of Melbourne and University of Southampton. Currently the two universities are in joint-research investigating ship-hull roughness and biofoulings (Utama et al. 2016). As previously mentioned, for large marine vehicle such as ships the majority of its drag penalty come from skin friction drag. The two most common source of roughness on ship are biofouling and the hull profile it-self.

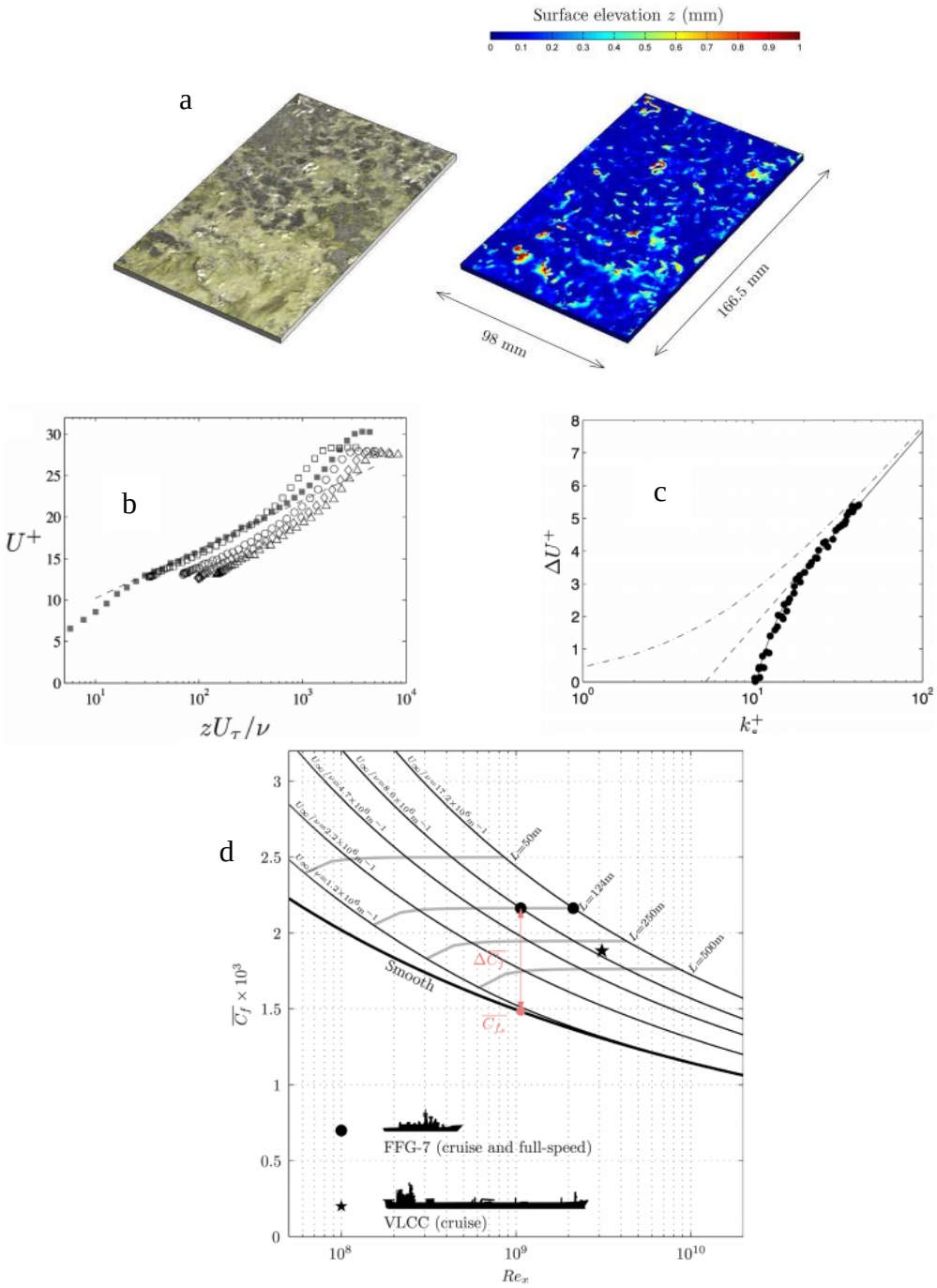

FIGURE 4: (a) fouled coupon photo and the laser scanning result; (b) mean velocity profiles of the rough surface at several Reynolds number; (c) ΔU^+ as function of k_s^+; (d) estimation increase of drag penalty for realistic scale ship. (Monty et al, 2016)

First we will discuss about biofouling, it is the settlement of marine creature on a surface in aquatic environment such as river, lake, or sea (Schultz, 2004; 2007; 2011). Recent study by Schultz (2011) show that the economic impact of biofouling towards the fleet of US navy's FFG-7 frigates is around $1bn over 15 years. Hence there is a pressing need to understand more about biofouling

and to predict full-scale ship drag penalty. Recently Monty et al. (2016) report a method to predict a full-scale ship drag penalty due to biofouling from laboratory experiment. In order to have realistic biofouling roughness they obtained a test coupon of biofouling (tubeworm) and then scanned using a laser triangulation sensor. The scan is then scaled and manufactured via CNC machine and copied using moulding and casting technique. The multiple casts are later laid onto the wind tunnel (filling the entire test section) and measured using hot-wire anemometer. The boundary layer measurement provides the necessary k_s values and it can be used to predict the drag penalty on full scale ship system (see figure 4).

The second type of roughness on marine transportation is from the hull surface itself. Although surface roughness on ship hull is generally associated with biofouling, many ships that have just recently cleaned, sand-blasted and repainted with anti-corrosion and anti-fouling paints during dry-dock also have noticeable rough-hull with height ranging from 0.1 – 0.5 mm. This surface roughness pattern is commonly termed as "orange-peel" pattern. Figure 5 shows the laser scanning result from a freshly cleaned and painted ship hull. We intend to perform similar study as Monty et al. (2016), using the orange peel pattern and to predict the drag penalty on the supposedly "clean ship hull", the laboratory experiment is currently still underway. Their initial estimation shows that even a recently dry docked ship hull will experience 22% drag penalty compared to hydrodynamically smooth wall.

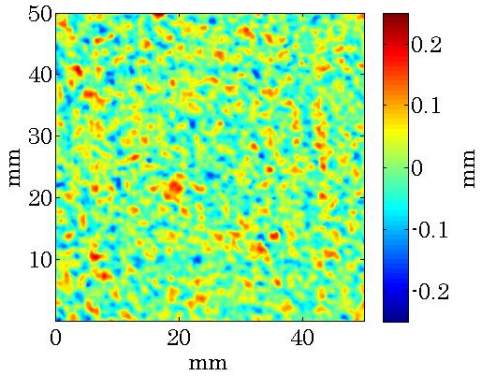

FIGURE 5: "Orange peel" pattern roughness from recently dry-docked ship

EXPERIMENTS ON AIRFOIL WITH DIRECTIONAL RIBLETS

A wind tunnel test to understand how roughness elements reduce drag have been conducted at Universiti Kebangsaan Malaysia (Harun et al. 2016). A purpose-built NACA 0026 airfoil has been fabricated using mostly wooden structure, plywood surface and stainless steel support. The chord, c is 600 mm and the span s_p is 500 mm. The thickness, t is 156 mm. The chord line falls on the mean camber line, therefore, this is a symmetrical airfoil. Wind tunnel test section bottom and top surface work as plates to minimize two-dimensionality issues. A 16 mm diameter stand, made of stainless steel is attached to one side of the airfoil to ensure a rigid support. The riblet surface was applied on one side of the airfoil using glue; this is shown by the black strip in figure 6. The length of the riblet surface is 50 mm. The riblets surfaces were applied here because of the needs of a sufficient length where the after-effect could develop in the boundary layer towards the rest of the airfoil (until the trailing edge).

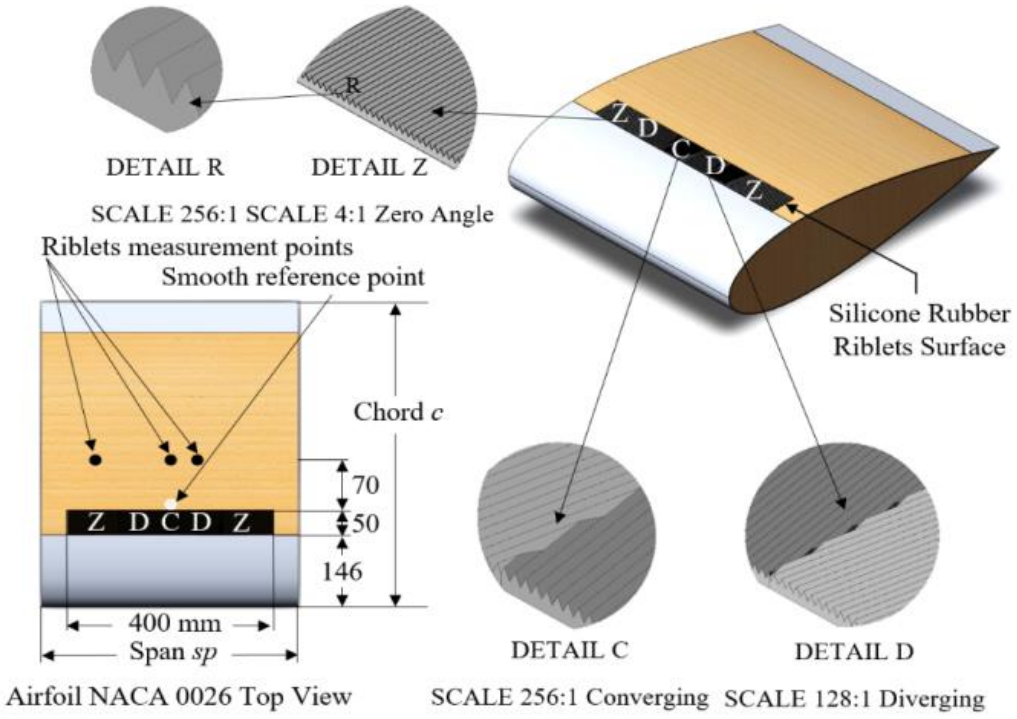

FIGURE 6: NACA 0026 airfoil dimension and application of riblet

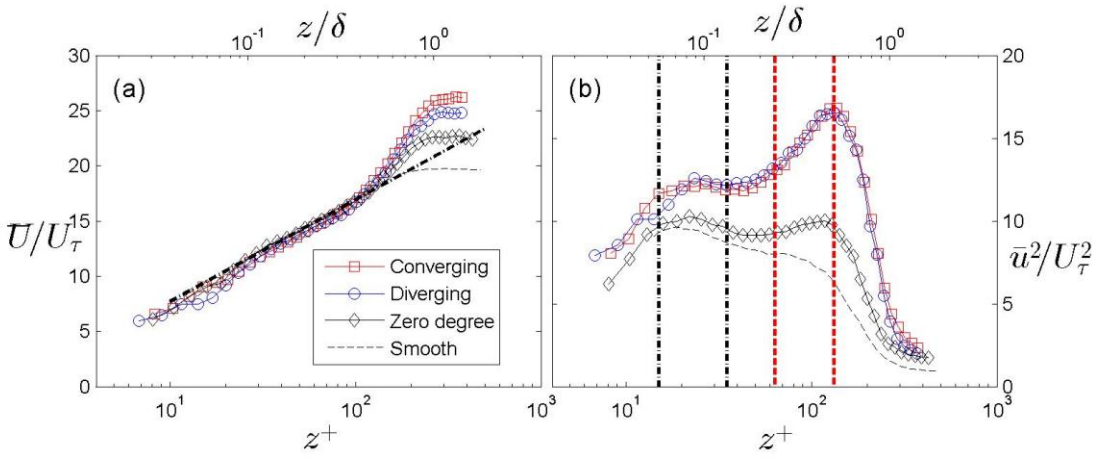

FIGURE 67 (a) Mean velocity profiles, the dashed-line indicates $1/\kappa \ln(z^+) + B$, here $\kappa = 0.25$, $B = -1.5$. (b) Turbulence intensities profile, dashed-dot black vertical lines indicate $z^+ = 15$ in the near wall region and $z^+ = 35$ at the start of logarithmic region. The dot-dashed red vertical lines indicate $3.9Re^{0.5}$ in the middle of logarithmic region and 0.5δ in the outer region respectively.

Figure 7(a) shows the velocity profiles of smooth wall reference flow, riblet arranged in the flow direction ($\alpha = 0^O$) and riblets arranged in converging and diverging directions ($\alpha = 10^O$). As expected, the velocity profile where a strip of riblet in converging direction applied, the boundary layer thickness thicken. This is remarkably different from the one where riblet is in the flow direction ($\alpha = 0^O$). Figure 7(b) turbulence intensities profiles. Riblets arranged in converging and

diverging direction produce similar inner and outer humps. The outer hump is remarkably larger than that for riblet arranged in the flow direction, this is shown by the red dashed line at 0.5δ.Similar pattern is observed in the middle of log region $3.9Re^{0.5}$. At z^+ =15 in the near wall region and z^+ =35 at the start of logarithmic region, turbulence intensities for both converging and diverging pattern are also larger than that for the riblet arrange in the direction of the flow. This suggest that the longer-scale structures actively influence the near-wall features i.e. similar to pressure gradient effects (Harun et. al. 2011; Harun et al. 2013).

To further understand this, the energy spectra analysis is provided. All representations of pre-multiplied energy spectra $k_x\varphi_{uu}$ are plotted against streamwise wavelength $\lambda_x = 2\pi/k_x$, where wave-number $k_x = 2\pi f/U_c$, f is the frequency and U_c is the convection velocity.

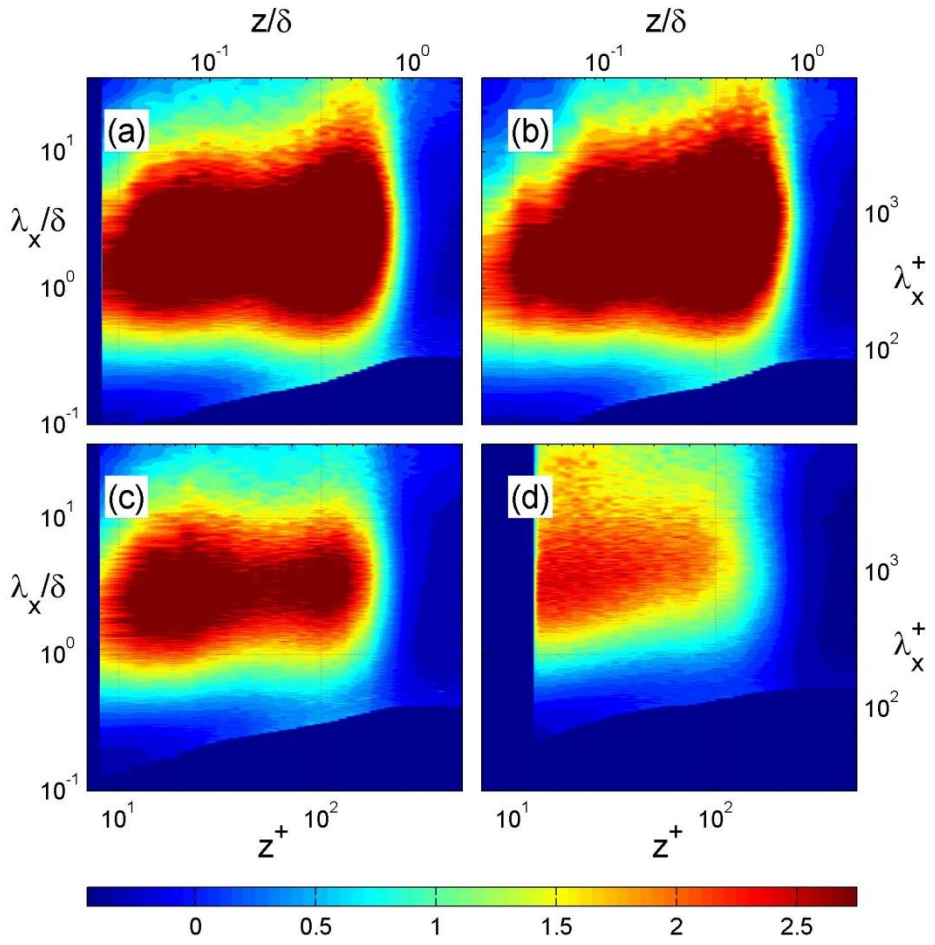

FIGURE 8: (a) Converging, (b) diverging, (c) zero degree and (d) smooth surface spectral map.

Figure 8(a-d) show energy spectra for all cases. It is clear now that riblets arranged in converging (8(a and b)) cause the longer-scale features are energized, in comparison with the riblets arranged in the flow direction (8(c)). Further analysis at z = 0.5δ reveals that the larger scale features dominating the outer hump are similar to the ones in wind tunnel studies i.e. 4-6δ. From the Clauser method, a strip of riblet arranged in converging and diverging direction cause the skin friction to reduce by 25%- 30%. An ongoing works are underway to apply these riblets with the Royal Navy of Malaysia to boost speeds of intercepting boats and provide more patrolling endurance.

SIMULATION WORKS ON ROUGH SURFACES

Conducting scaled laboratory experiments are expensive as it requires very specialised equipment and facilities. Fabricating the rough surface to be tested in a wind tunnel is also a tedious and time consuming procedure. With the advancement of computational power, there has been much focus on using computational fluid dynamics (CFD) to simulation turbulent flows over rough surfaces. Direct numerical simulation (DNS) is a method where the governing equations of fluid flow is directly solved without any averaging or modelling. Therefore, an accurate representation of the flow can be simulated. The advantage of DNS is that the volumetric and time resolved information of the flow are readily available which is extremely difficult to obtain when conducting laboratory experiments. Throughout the years, there has been extensive work which aims to better understand the turbulent flow over roughness of various shapes and configurations (Busse et al. 2017; Orlandi & Leonardi, 2006; Orlandi et al. 2006; Yuan & Piomelli 2014).

Recent works by Chan et al. (2015) and MacDonald et al. (2016) showed the effects of solidity Λ which is the ratio of the frontal area to the planar area of the roughness. Λ is an important roughness parameter and has a large impact on the value of ΔU^+. For sparse roughness ($\Lambda < 0.15$), ΔU^+ increases with increasing Λ. On the contrary, in the dense regime ($\Lambda > 0.15$), ΔU^+ decreases with increasing Λ. Figure 9 illustrates the sketches of a rough wall pipe which consist of three-dimensional sinusoidal roughness elements of varying solidity. At the limits when $\Lambda \to 0$, the rough wall will approach a smooth wall and when $\Lambda \to \infty$, the rough wall will also approach a smooth wall but with a shifted wall-normal height.

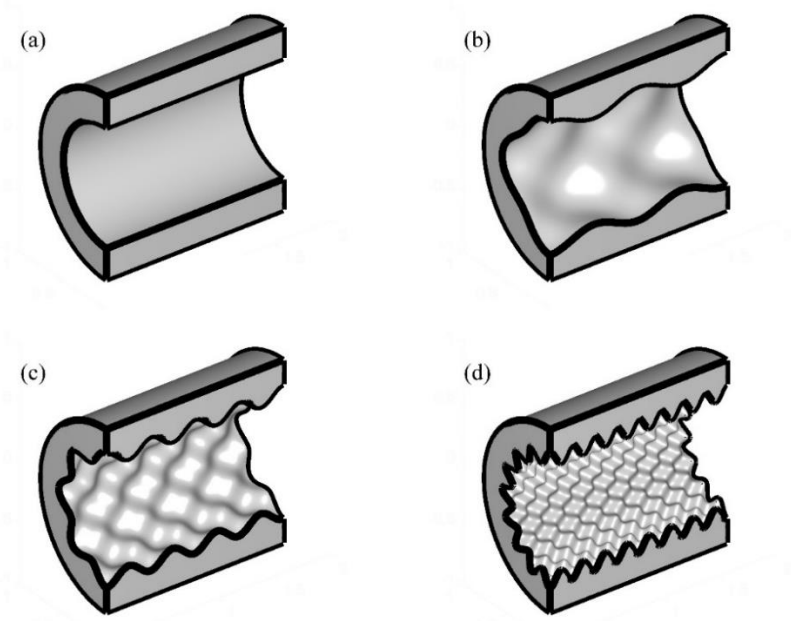

FIGURE 9: Sketch of (a) smooth pipe and rough pipes with three-dimensional sinusoidal roughness elements in a pipe with (b) $\Lambda = 0.09$ (sparse roughness), (c) $\Lambda = 0.18$ (dense roughness) and (d) $\Lambda = 0.36$ (dense roughness).

ROUGHNESS FUNCTION MODELS

While accurate results can be obtained via CFD, current computational resources only allows for flows at moderate Reynolds number to be simulated as the computational requirements scales with the $Re^{9/4}$. This requirement could potentially be much larger for turbulent flow over rough

surfaces as the computational mesh not only needs to resolve the Kolmogorov scales (the smallest turbulent eddies in the flow) but also the topology of the roughness. There has been attempts to reduce the computational cost of these simulations by conducting minimal channel simulations whereby the spanwise length of the domain is smaller than a typically sized channel (Chung, et al. 2015; MacDonald et al., 2017). Despite the reduction in computational cost, the Reynolds number of the flow is still significantly lower than that observed in engineering flows.

Therefore, for practical engineering applications, conducting CFD or laboratory experiments are unfeasible. Rather, empirical models have to be used so that engineers are able to obtain a quick estimate of the drag penalty of the surface. One of the most commonly used tool in estimating the drag of a rough surface is the Moody's diagram. With the Moody's diagram, an engineer is able to predict the drag of a rough surface if the operational Reynolds number, the relative roughness and the equivalent height of the roughness is known. The downside of the Moody's diagram is that it is inaccurate and over predicts the drag especially when the flow is in the transitionally rough regime (Allen et al. 2005; Langelandsvik, et al. 2008).

Empirical models called roughness function models attempts to relate the topological features of the rough surface to its drag penalty. These models aim to predict the drag of a surface by considering the effects of one or more roughness parameters. Flack & Schultz (2010) reviews some of the previously proposed roughness function models. They also suggested that the drag of a surface (or ΔU^+) depends on the root-mean-squared of the roughness k_{rms}^+ and also the skewness of the roughness k_{skew}^+. While it was found that their model was able to accurately predict the ΔU^+ value for sandgrain and gravel type roughness, it did not perform well for small roughnesses found in the honed and commercial steel pipes. Another roughness function model developed was by Chan et al. (2015) who proposed a correlation based on the average roughness height k_a^+ and the effective slope ES (which is analogous to solidity, $ES = 2\Lambda$),

$$\Delta U_{est}^+ = \alpha \log(k_a^+) + \beta \log(ES) + \gamma \quad (4)$$

where ΔU_{est}^+ is the roughness function predicted by the model and $\alpha = 1/\kappa$, $\beta = 1.12$ and $\gamma = 1.47$ are empirical constants based on the rough wall pipe simulations. This roughness function model has been used by Hutchins et. al. (2016) and is able to accurately predict the drag of a surface populated with tubeworm biofouling (see figure 4a). This simplistic model however, does not take into consideration the effects of the alignment and sheltering of the roughness elements. None of the roughness function models proposed have been universally applicable and breaks down for certain types of roughness configuration.

CONCLUSION

While there has been much knowledge acquired in this field of research in recent years, there is still many aspects of the turbulent flows over rough surfaces which has yet to be fully understood. Nevertheless, theory on riblets to reduce drags on super tanker have been put into physical installation because small change could significantly alter overall ship's fuel consumption in one complete international trip. Studies in lab-scale and field works have to be carried out rigorously to confirm actual drags. In many parts, when experimental works are just unjustifiably costly, simulation works have to be carried out. These works have proven to be very beneficial to the mankind as the fuel efficiency not only save billions of dollar in a year, but also emission are decreased indirectly.

ACKNOWLEDGEMENTS

This work was supported by the Research Fund provided by The Ministry of Higher Education Malaysia via grant FRGS/2016/TK03/UKM/02/1/ and UKM grant AP-2015-003.

REFERENCES

Acharya, A., Bornstein, J., Escudier, M.P., 1986. Turbulent boundary layers on rough surfaces. *Exp. Fluids* 4, pp. 33 – 47.

Aftab, S.M.A, Razak, N.A, Rafie, A.M. and Ahmad K.A., 2016. Mimicking the humpback whale: An aerodynamic perspective, *Prog. in Aerospace Sciences* 84, pp. 48-69.

Allen, J.J., Shockling, M.A., & Smits, A.J. 2005. Evaluation of a universal transitional resistance diagram for pipes with honed surfaces. *Phys. of Fluids* (1994-Present), 17(12): 121702.

Amir, M., Castro, I. P., 2011. Turbulence in rough-wall boundary layers: universality issues. *Phys. Fluids* 51, pp. 313 – 326.

Baars, W.J., Squire, D.T., Talluru, K.M., Abbassi, M.R., Hutchins, N., Marusic, I. 2016. Wall-drag measurements of smooth- and rough-wall turbulent boundary layers using a floating element. *Exp. Fluids*, 57(90): 1-16.

Busse, A., Thakkar, M., and Sandham, N.D. 2017. Reynolds-number dependence of the near-wall flow over irregular rough surfaces. *J. Fluid Mech.* 810, pp. 196–224.

Chan, L., MacDonald, M., Chung, D., Hutchins, N., & Ooi, A. 2015. A systematic investigation of roughness height and wavelength in turbulent pipe flow in the transitionally rough regime. *J. Fluid Mech.* 771, pp. 743–777.

Chung, D., Chan, L., MacDonald, M., Hutchins, N., & Ooi, A. 2015. A fast direct numerical simulation method for characterising hydraulic roughness. *J. Fluid Mech.* 773, 418–431.

Chen, H., Rao, F., Shang, X., Zhang, D. and Hagiwara, I. 2013. Biomimetic drag reduction study on herringbone riblets of bird feather, *J. of Bionic Engineering* 10(3) pp. 341-349.

Clauser, F.H., 1954. Turbulent boundary layers in adverse pressure gradients. *J. Aeronaut. Sci.* 21, pp. 91–108.

Dean, B. & Bhushan, B. 2010. Shark-skin surfaces for fluid-drag reduction in turbulent flow: a review. *Phil. Trans. R. Soc. of London A*, 368(1929) pp. 4775 – 4806.

Flack, K.A. & Schultz, M.P. 2010. Review of hydraulic roughness scales in the fully rough regime. *J.of Fluids Eng.* 132(4): 041203.

Foon, H.W. 2017. Giant Carey Island port in the works, http://www.thestar.com.my/news/nation/2017/01/09 /giant-careyisland- port-in-the-works-massive-project-with-rm200bil-in-investments-will-cover-100-sq/, retrieved 7 Jan. 2017.

Harun, Z., Abbas, A. A, Mohammed Dheyaa, R. and Ghazali, M. I., 2016, Ordered roughness effects on NACA 0026 airfoil. *J. of Physics Conference Series: Mtrls. Sc. and Eng*. 152, 012005.

Harun, Z., W. Ghopa, W.A., Abdullah, A., Ghazali, M.I., Abbas, A.A., Rasani, M.R., Zulkifli, Z., Wan Mahmood, W.M.F., Abu Mansor, M.R., Zainol Abidin, Z., Wan Mohtar, W.H.M. 2016. The development of a multi-purpose wind tunnel. *J. Teknologi* 78(6-10): 63-70.

Harun, Z., Monty J.P., Mathis, R. and Marusic, I. 2013. Pressure gradient effects on the large-scale structure of turbulent boundary layers *J. of Fluid Mech.* 715 pp. 477-498.

Harun, Z., Monty J.P. and Marusic, I. 2011. The structure of zero, favorable and adverse pressure gradient turbulent boundary layers, *TSFP Digital Library Online*. Begel House Inc.

Hutchins, N., Monty, J.P., Nugroho, B., Ganapathisubramani, B., & Utama, I. 2016. Turbulent boundary layers developing over rough surfaces: from the laboratory to full-scale systems.

Igaz, S. 2016. Major oil spill in Malaysian port Tanjung Pelepas, 2016, Maritime Herald, http://www.maritimeherald.com/2016/major-oil-spill-in malaysian-port-tanjung-pelepas-closed-container-terminal/, retrieved 7 Jan. 2017.

Khoo, S., 2016. Kuantan Port expansion to improve economic ties with China, *The Star Online*, 14 February 2015, http://www.thestar.com.my/ news/nation/2015/02/14/ kuantan-port-expansion-to-improve-economic-ties-with-china/, retrieved 7 Jan. 2017.Koeltzsch, K.,

Dinkelacker, A. and Grundmann R, 2002, Flow over convergent and divergent wall riblets. *Exp. in Fluids* 33(2) pp 346-350.

Krogstad, P.-A., Antonia, R.A., 1999. Surface roughness effects in turbulent boundary layers. *Exp. Fluids* 27, pp. 450 – 460.

Langelandsvik, L.I., Kunkel, G.J., and Smits, A J. 2008. Flow in a commercial steel pipe. *J. Fluid Mech.* 595, pp. 323–339.

Lee, J.H., Sung, H.J. and Krogstad P-A, 2011. Direct numerical simulation of the turbulent boundary layer over a cube-roughened wall *J. Fluid Mech.* 669 pp. 397 – 431.

Ligrani, P. M., Moffat, R. J., 1986. Structure of transitionally rough and fully rough turbulent boundary layers. *J. Fluid Mech* 162, pp. 69 – 98.

Luo, Y., Yuan, L., Li, J. and Wang, J. 2015. Boundary layer drag reduction research hypotheses derived from bio-inspired surface and recent advanced applications *Micron* 79 pp. 59-73.

MacDonald, M., Chan, L., Chung, D., Hutchins, N., & Ooi, A. 2016. Turbulent flow over transitionally rough surfaces with varying roughness densities. *J. Fluid Mech.* 804, pp. 130–161.

MacDonald, M., Chung, D., Hutchins, N., Chan, L., Ooi, A., & García-Mayoral, R. 2017. The minimal-span channel for rough-wall turbulent flows. *J. Fluid Mech.* 816, pp. 5–42.

Marusic, I., Mathis, R. and Hutchins, N. 2010. High Reynolds number effects in wall turbulence. *Intl. J. of Heat and Fluid Flow* 31 pp. 418–428.

Monty, J.P., Dogan, E., Hanson, R., Scardino A.J., Ganapathisubramani, B. and Hutchins, N. 2016. An assessment of the ship drag penalty arising from light calcareous tubeworm fouling. Biofouling, 32(4): 451-64.

Nugroho, B., Hutchins, N. and Monty, J.P. 2013, Large-scale spanwise periodicity in a turbulent boundary layer induced by highly ordered and directional surface roughness. *Int. J. of Heat and Fluid Flows* vol. 41, pp. 90–102.

Nikuradse, J. 1933. Laws of Flow in Rough Pipes, NACA Technical Memorandum 1292.

Orlandi, P., & Leonardi, S. 2006. DNS of turbulent channel flows with two- and three-dimensional roughness. Journal of Turbulence, 7, N73.

Orlandi, P., Leonardi, S., & Antonia, R. A. 2006. Turbulent channel flow with either transverse or longitudinal roughness elements on one wall. *J. Fluid Mech.*, 561, pp. 279–305.

Perry, A. E., Schofield, W.H., and Joubert, P.N., 1969. Rough wall turbulent boundary layers. *J. Fluid Mech.* 37, pp. 383 – 413.

Reuters. 2017. Chinese-backed Port City in Sri Lanka to attract $13bn in investment from 2018, https://www.dawn.com/news/1323981, retrieved 4 April 2017.

Saric, W.S., Carpenter, A.L. and Reed, H.L., 2011. Passive control of transition in three-dimensional boundary layers, with emphasis on discrete roughness elements, *Phil. Trans. R. Soc. A* 369 pp. 1352 – 1364.

Stenzel, V., Wilke. Y. and Hage, W. 2011. Drag-reducing paints for the reduction of fuel consumption in aviation and shipping *Prog. Organic Coatings* 70 pp. 224–229.

Smits, A.J. & Marusic, I, 2013. Wall-bounded turbulence *Physics Today* 66 pp. 25 – 30.

Theguardian, 2016, True scale of CO_2 emissions from shipping revealed.

Perry, A.E. & Li, J.D., 1990. Experimental support for the attached-eddy hypothesis in zero-pressure-gradient turbulent boundary layers. *J. Fluid Mech*. 218, 405–438.

Schultz, M.P. 2004. Frictional resistance of antifouling coating systems. *ASME J Fluids Eng.* 126, pp. 1039 – 1047.

Schultz, M.P. 2007. Effects of coating roughness and bio-fouling on ship resistance and powering. Bio-fouling 23(5-6): 331–341.

Schultz, M.P, Bendick, J.A., Holm, E.R. and Hertel, W.M. (2011) Economic impact of biofouling on a naval surface ship. *Biofouling* 27 pp. 87-98.

Smits, A.J., McKeon, B.J., Marusic, I., 2011. High Reynolds number wall turbulence. *Annu. Rev. Fluid Mech*. 43 pp. 353–375.

Squire, D.T., Morrill-Winter, C., Hutchins, N., Schultz, MP., Klewicki J.C., and Marusic I. 2016a. Comparison of turbulent boundary layers over smooth and rough surfaces up to high Reynolds numbers. *J. Fluid Mech.* 795, pp. 210-240.

Squire, D.T., Morrill-Winter, C., Hutchins, N., and Marusic I. 2016b. Smooth-and rough-wall boundary layer structure from high spatial range particle image velocimetry. *Phys. Rev. Fluids 1* 064402.

Utama, I. K. A. P., Ganapathisubramani, B., Hutchins, N., Nugroho, B., Monty, J.P., Prasetyo, F. A., Yusuf, M., Tullberg, M. 2016. International collaborative work to improve research quality and enhance academic achievement. The Royal Institution of Naval Architects (RINA) Education & Professional Development of Engineers in the Maritime Industry Conference, Singapore.

Volino, R.J., Schultz, M.P., Flack, K.A., 2009. Turbulence structure in a boundary layer with two-dimensional roughness. *J. Fluid Mech.* 635, pp. 75 – 101.

Yuan, J., & Piomelli, U. 2014. Estimation and prediction of the roughness function on realistic surfaces. *J. of Turbulence*, 15(6): 350–365.

Zambri Harun

Department of Mechanical & Materials Engineering,
Unversiti Kebangsaan Malaysia,
43600 UKM Bangi, Malaysia
Phone: + 603 – 8921 6518
Email address: zambri@ukm.edu.my